Science Background for the Reprocessing and Goddard Satellite-based Surface Turbulent Fluxes (GSSTF2b) Data Set for Global Water and Energy Cycle Research

Version 1.0

Release Date: October 12, 2010

Goddard Earth Sciences Data and Information Services Center (GES DISC)
http://disc.gsfc.nasa.gov
NASA Goddard Space Flight Center
Code 610.2
Greenbelt, MD 20771 USA

Science Background for the Reprocessing and Goddard Satellite-based Surface Turbulent Fluxes (GSSTF2b) Data Set for Global Water and Energy Cycle Research

The global water cycle's provision of water to terrestrial storage, reservoirs, and rivers rests upon the global excess of evaporation to precipitation over the oceans. Variations in the magnitude of this ocean evaporation excess will ultimately lead to variations in the amount of freshwater that is transported (by the atmosphere) and precipitated over continental regions. The air-sea fluxes of momentum, radiation, and freshwater (precipitation – evaporation) play a very essential role in a wide variety of atmospheric and oceanic problems (e.g., oceanic evaporation contributes to the net fresh water input to the oceans and drives the upper ocean density structure and consequently the circulation of the oceans). Information on these fluxes is crucial in understanding the interactions between the atmosphere and oceans, global energy, and water cycle variability, and in improving model simulations of climate variations.

Document maintained by *GES DISC Personnel*

Approved by: Andrey K. Savtchenko

Dataset Provider: Goddard Earth Sciences Data and Information Services Center
Dataset Provider Address: Code 610.2, NASA Goddard Space Flight Center, Greenbelt Rd., Greenbelt, MD 20771, USA

Table of Contents

1. Introduction

This document provides basic information for using Goddard Satellite-based Surface Turbulent Fluxes Version 2b (a.k.a. GSSTF2b) Data Set products.

The GSSTF2b (July 1987-December 2008) consists of products generated for the focus on Global Water and Energy Cycle Research. The global water cycle's provision of water to terrestrial storage, reservoirs, and rivers rests upon the global excess of evaporation to precipitation over the oceans. Variations in the magnitude of this ocean evaporation excess will ultimately lead to variations in the amount of freshwater that is transported (by the atmosphere) and precipitated over continental regions. The air-sea fluxes of momentum, radiation, and freshwater (precipitation – evaporation) play a very essential role in a wide variety of atmospheric and oceanic problems (e.g., oceanic evaporation contributes to the net fresh water input to the oceans and drives the upper ocean density structure and consequently the circulation of the oceans). Information on these fluxes is crucial in understanding the interactions between the atmosphere and oceans, global energy, and water cycle variability, and in improving model simulations of climate variations.

2. Overview and Background

2.1 Product/Algorithm Objectives

The previous GSSTF dataset (GSSTF2; July 1987-December 2000) has been widely used by scientific communities for global energy and water cycle research and regional and short period data analysis since its official release in 2001. The objective of this project is to continually produce a uniform data set of sea surface turbulent fluxes (i.e., latent heat flux, sensible heat flux and wind stress) derived from remote sensing data (SSM/I) and reanalysis (NCEP) that would continue to be useful for global energy and water flux research and applications. We are looking forward to serving the scientific communities with another useful dataset in GSSTF2b.

2.2 Historic Perspective

Accurate sea surface fluxes measurements are crucial to understanding the global water and energy cycles. The oceanic evaporation that is a major component of the global oceanic fresh water flux is particularly useful to predicting oceanic circulation and transport. Our previous GSSTF2 product (Chou et al. 2001; Chou et al. 2003) has been widely used by scientific communities for global energy and

water cycle research and regional and short period data analysis since its official release in 2001 by NASA/GSFC DISC. Our records (mostly based on personal communications) indicate almost 30 communities using GSSTF2 (our previous version dataset) for scientific research during a six-year (2001-2006) period, not to mention the SEAFLUX Project and those who might have attained GSSTF2 directly from the DISC website. Numerous GSSTF2-related research studies were published in journals or presented in conference meetings, which may be readily fetched via the web search engines. The users range from US government agency (e.g., NASA/GSFC, GISS, LRC, MSFC, and NOAA) to universities and institutes from different countries (e.g., Colorado State U., Columbia U., George Mason U., IAP/Chinese Academy of Sci. in China, MIT, National Taiwan U., UMBC, UMCP, U. of Massachusetts, U. of Tokai/Japan, U. of Washington, Woods Hole Ocea. Institution). The datasets were used for various scientific objectives. However, the GSSTF2 product ended in 2000.

A new version of GSSTFT product, i.e., GSSTF2b has therefore been revived/produced and brought up-to-date using improved input data sets, i.e., surface/10-m wind speeds (U), total precipitable water (W), bottom-layer (500 m) precipitable water (WB) of the SSM/I V6, and SST, 2-m air temperature (Ta), and sea level pressure (SLP) of the NCEP/DOE Reanalysis-2 (R2). The input datasets previously used for producing GSSTF2 were products of the SSM/I V4 and the NCEP R1. Moreover, a recently upgraded Cross-Calibrated Multi-Platform (CCMP) ocean surface wind vector product (Atlas et al., 2009), which was based on the same variational analysis method (VAM) applied for producing an earlier surface wind vector dataset (Atlas et al., 1996) used for determining the GSSTF2 wind stress vectors, has been used for the GSSTF2b production. Detailed info’s on GSSTF2b can also be found in Shie et al. (2009) and Shie et al. (2010).

2.3 Data Product Characteristics

There are two sets of GSSTF2b, i.e., "Set1" and "Set2" (July 1987-December 2008), respectively. They are both “Combined” data, but different for being produced using a different combination of individual satellite products. Set1/Set2 may contain a larger/smaller global temporal trend in latent heat flux, but with less/more missing data. They are stored together in HDF-EOS5 files, under two separate Grids, SET1 and SET2.

The GSSTF2b, daily fluxes have first been produced for each individual available SSM/I (Special Sensor Microwave Imager) satellite tapes (e.g., F08, F10, F11, F13, F14 and F15). Then, the Combined daily fluxes are produced by averaging (equally weighted) over available flux data/files from various satellites. These Combined daily flux data are considered as the "final" GSSTF2b, and are stored in this HDF-EOS5 collection. Data should be used with care and proper citations, i.e., properly indicating your applications with, e.g., "using the combined 2001 data file of Set1 (or Set2)" or "using the 2001 F13 data file". Set1 (involved with more satellite data) does not necessarily possess better real data quality than Set2. The users may feel free to use either Set1 or Set2 with their own interests and justifications (likewise, they may also use the product of individual satellites).

The MEaSUREs project at GES DISC, however, converted all data into HDF-EOS5 format and reorganized it into separate daily and monthly files, in a manner consistent with the on-going Earth Observing System (EOS) missions such as Aura, Aqua, and Terra. The monthly, seasonal and yearly climatologies are also in HDSF-EOS5 format, in separate files. I.e. the daily files are now easily searchable and downloadable by data day.

The essential meaning of HDF-EOS5 is that the data are now in a standard “Grid” format. The Set1 and Set2 eight major variables are grouped into two separate grids, named “SET1” and “SET2”, and the two grids are stored together in one file. Further, the “minor” variable - total precipitable water - is grouped together with the eight major variables in the corresponding SET1 or SET2 grid. Thus each grid contains 9 variables. This organization is identical for all daily and monthly files, apart from the model reanalysis. The “common”, NCEP/DOE Reanalysis II, data are stored in separate files with one Grid containing the four “common” variables. The climatologies (monthly, seasonal, and yearly) also contain the SET1 and SET2 grids, but in addition are also containing the four NCEP variables in a separate grid.

The “individual tapes” representing the individual SSM/I satellites are stored in separate collections and daily files, one day per file. They contain one grid that is named on the satellite name (F08, F10, F11, F13, F14, and F15). The grid contains the nine variables (8 major + 1 minor) that go into the computation of the final nine “combined” retrieved variables.

All data within these HDF-EOS5 are easily recognizable as 360x180 arrays, representing global map, at 1x1 deg grid cell size. The endianness of the remote storage and the users’ local machines become irrelevant. The concept of headers and offsets, typical for the binary format, disappears and all that matters are Grid and data field names that are very easy to list out using command line utilities.

This data organization results in 13 data types, with Short Names listed below. The Short Name is the first string in all filenames, and it is also stored inside the files as a global file attribute “ShortName”.

<u>A. Daily:</u>
There are total of Eight (8) daily data types.

GSSTF
GSSTF_NCEP
GSSTF_F08
GSSTF_F10
GSSTF_F11
GSSTF_F13
GSSTF_F14
GSSTF_F15

1) GSSTF
It has 2 grids, "SET1" and "SET2". Every grid has 9 parameters, the 8 "major" plus the "minor" total precipitable water.

2) GSSTF_NCEP
It has one grid, "NCEP", with 4 parameters. The original were the "common" binary files, that is the NCEP/DOE Reanalysis II.

3) GSSTF_Fxx

These are the individual satellites, where Fxx is one of the following (F08, F10, F11, F13, F14, and F15). The HDF-EOS5 files have only one grid which takes the name of the individual satellite. Every grid has 9 parameters, the 8 "major" plus the "minor" total precipitable water.

B. Monthly:

There are two Monthly data types in he5.
GSSTFM
GSSTFM_NCEP

1) GSSTFM

It has four (4) grids: SET1, SET1_INT, and SET2, SET2_INT, where "INT" stands for interpolated. Each of these has 9 (nine) parameters: the 8 "major" plus the "minor" total precipitable water.

2)GSSTFM_NCEP

This is the "common" monthly NCEP/DOE Reanalysis II. It has one grid with four parameters.

C. Climatology

There are three (3) climatological data types: Monthly, Seasonal, and Yearly in HDF-EOS5:
GSSTFMC
GSSTFSC
GSSTFYC

The climatologies (monthly, seasonal, and yearly) also contain the SET1 and SET2 grids, but in addition are also containing the four NCEP/DOE Reanalysis II variables in a separate grid, “NCEP”.

Summary of All Data Types:

GSSTF
GSSTF_NCEP
GSSTF_F08
GSSTF_F10
GSSTF_F11
GSSTF_F13
GSSTF_F14
GSSTF_F15
GSSTFM
GSSTFM_NCEP
GSSTFMC
GSSTFSC
GSSTFYC

The file naming convention for the non-climatological HDF-EOS5 files produced at GES DISC for the GSSTF2b project is as follows:

ShortName.vv.yyyy.mm.dd.he5

Where:

- ShortName = one of the following Data Types:
  GSSTF
  GSSTF_NCEP
  GSSTF_F08
  GSSTF_F10
  GSSTF_F11
  GSSTF_F13
  GSSTF_F14
  GSSTF_F15
  GSSTFM
  GSSTFM_NCEP
  GSSTFMC
  GSSTFSC
  GSSTFYC

- vv = 2b for this release
- yyyy = data year
- mm= data month
- dd = start date for the data
- he5 = commonly accepted extension for HDF-EOS5 files.

Filename example for the daily "combined" turbulent fluxes retrieval, for November 1, 2000:
GSSTF.2b.2000.11.01.he5

Climatologies have slightly different file names that reflect the Month (for monthlies), and the range of Months (for seasonal), and the range of years for which the climatology is built. The yearly climatology has one file only.

Example file name for Monthly climatology for November:

GSSTFMC.2b.Nov.1988_2008.he5

Example file name for seasonal climatology for September-November:

GSSTFSC.2b.Sep_Nov.1988_2008.he5

Each **SET1** or **SET2** grid (including interpolated, SET1_INT, SET2_INT) contains the following 9 science data fields:

data_field_short_name	Data field long name (units)
"E"	'latent heat flux' (W/m**2)
"STu"	'zonal wind stress' (N/m**2)
"STv"	'meridional wind stress' (N/m**2)
"H"	'sensible heat flux' (W/m**2)
"Qair"	'surface air (~10-m) specific humidity' (g/kg)
"WB"	'lowest 500-m precipitable water' (g/cm**2)
"U"	'10-m wind speed' (m/s)
"DQ"	'sea-air humidity difference' (g/kg)
"Tot_Precip_Water"	'total precipitable water' (g/cm**2)

Each NCEP Grid contains the following 4 data fields:

Data field short name	Data field long name (units)
"SST"	'sea surface skin temperature' (C)
"Psea_level"	'sea level pressure' (hPa)
"Tair_2m"	'2m air temperature' (C)
"Qsat"	'sea surface saturation humidity' (g/kg)

3. Physics of the Problem

The Earth's climate is characterized by a myriad of processes that couple the ocean, land, and atmosphere systems. The global water cycle's provision of water to terrestrial storage, reservoirs, and rivers rests upon the global excess of evaporation to precipitation over the oceans. Variations in the magnitude of this ocean evaporation excess will ultimately lead to variations in the amount of freshwater that is transported (by the atmosphere) and precipitated over continental regions. The air-sea fluxes of momentum, radiation, and freshwater (precipitation – evaporation) play a very essential role in a wide variety of atmospheric and oceanic problems. Information on these fluxes is crucial in understanding the interactions between the atmosphere and oceans, global energy, and water cycle variability, and in improving model simulations of climate variations. These fluxes are thus required for driving ocean models and validating coupled ocean–atmosphere global models. Surface measurements of these fluxes are scarce in both space and time, especially over the oceans and in remote land areas. The Comprehensive Ocean–Atmosphere Data Set (COADS) has collected the most complete surface marine observations since 1854, mainly from merchant ships (Woodruff et al. 1993). However, the air–sea fluxes and input variables based on COADS have serious spatial and temporal sampling problems plus measurement uncertainty. It is, therefore, desirable that long-term global datasets of these fluxes

be derived either from satellite observations or general circulation models (GCMs). Indeed, satellite measurements nicely complement conventional data to provide or improve space/time estimates of many hydrologic parameters. Several efforts have been made to prepare datasets of ocean surface turbulent fluxes from satellite observations using bulk flux models. The SSM/I on board a series of Defense Meteorological Satellite Program (DMSP) satellites spacecraft has provided global radiance measurements for sensing the atmosphere and the surface. A number of techniques have been developed to derive the turbulent fluxes using parameters such as the surface air humidity and winds inferred from the SSM/I radiances (e.g., Chou et al., 1997: Schulz et al., 1997; Curry et al., 1999; Kubota et al., 2002).

4. Retrieval Algorithms

4.1 Ancillary Data Requirements

The GSSTF2b fluxes are produced using the up-to-date and improved input data sets, i.e., surface/10-m wind speeds (U), total precipitable water (W), bottom-layer (500 m) precipitable water (WB) of the SSM/I V6, and SST, 2-m air temperature (Ta), and sea level pressure (SLP) of the NCEP/DOE Reanalysis-2 (R2). WB that is derived from SSM/I brightness temperature (TB) following Schultz et al. (1993) is then, along with W, used to retrieve surface air (~10m) specific humidity (Qair) using the first two vertical EOFs of First Global Atmospheric Research Programme (GARP) Global Experiment (FGGE) IIb humidity soundings of six W-based climatic regimes over global oceans during December 1978–November 1979 (Chou et al. 1995 and Chou et al. 1997). Qair and Qs (surface saturation specific humidity based on SST), SST, Ta and U are eventually applied in the GSSTF bulk flux model/algorithm to produce the three air-sea turbulent fluxes, i.e., wind stress (τ), sensible heat flux (H), and latent heat flux (E). Moreover, the CCMP ocean surface wind vector is used to partition τ into the respective wind stress vectors, i.e., STu and STv.

4.2 Calibration and Validation

The SSM/I V4 surface wind speeds used for the previous GSSTF2 production was found carrying a linear trend of 6% increase in a 13.5-year period (Xing 2006). Remote Sensing Service (RSS) removed such spurious trends in its latest issued SSM/I V6 product. Shie et al. (2009) showed a consistent improvement in the surface wind speed from SSM/I V4 to V6 by comparing the respective daily V6 and V4 (combined F13 and F14) surface wind speeds of a 46-day period (i.e., 28 July - 11 September 1999) with the corresponding Kwajalein Experiment (KWAJEX) in situ observed wind speeds. Statistics indicated a rising correlation coefficient from 0.84 (V4) to 0.89 (V6), a significant reduction of root-mean-square (RMS)/stand-deviation-error (SDE) from 0.90/0.90 (V4) to 0.69/0.79 m s^{-1} (V6), and an

improved bias reduced from 0.15 (V4) to 0.10 m s^{-1} (V6). SDE is the standard deviation of the differences between the computed and observed. An extended validation on the SSM/I surface wind speed has been further conducted by including four more field experiments (Shie et al. 2010). A table listed below shows the periods and locations of these five 1999 experiments, i.e., KWAJEX, the Joint Air–Sea Monsoon Interaction Experiment (JASMINE), the buoy service in the North Pacific (MOORINGS), the Nauru'99 (NAURU99), and the Pan–American Climate Study in the eastern Pacific during 1999 (PACSF99). Similar to the aforementioned finding from KWAJEX, SSM/I wind speeds are also found improved (i.e., closer to the observed) from V4 to V6 for JASMINE, MOORINGS, and PACSF99. Statistics show a commonly reduced RMS, SDE, and bias for these three experiments, while correlation coefficient increases by a considerable amount of 0.11 (i.e., from 0.77/V4 to 0.88/V6) for MOORINGS. However, the V6 wind speed performs poorly for NAURU with even a negative correlation coefficient that costly turns around an otherwise overall better performance in V6. The supposedly trend-removed V6 wind speeds have indeed shown a general improvement in four of our five targeted experiments, yet still cannot guarantee a common improvement for each individual of the five experiments.

Table Times and locations of five field experiments conducted in 1999 by the NOAA/ETL research ships.

Field Experiments	Times	Locations
JASMINE	4–31 May 99	5^0S–13^0N, 88^0–98^0E
KWAJEX	28 Jul–10 Sep 99	9^0N, 167^0E
MOORINGS	14 Sep–21 Oct 99	8^0N, 167^0E–49^0N, 130^0W
NAURU99	15 Jun–18 Jul 99	12^0S, 130^0E–8^0N, 167^0E
PACSF99	2 Nov–1 Dec 99	8^0S–12^0N, 95^0–121^0W

The SSMI/I W and WB that are used to retrieve Qair using an EOF method (Chou et al. 1995) are, however, found varied insignificantly from V4 to V6, unlike what has been found in surface wind speed. The daily W of SSM/I V6 vs. V4 (combined F13 and F14; collected by collocating with the same set of sample observations consisting of the five field experiments) has a very close distribution with a correlation of 0.999, while V6 is slightly larger than V4 with a positive bias of 0.22 g kg-1 relative to a V4 mean of 45.36 g kg-1. Similar to W, the associated daily WB (V6 vs. V4) demonstrates a similar and consistent feature (with a correlation of 0.996) that V6 is slightly larger than V4 with a positive bias of 0.015 g kg-1 relative to a V4 mean of 0.995 g kg-1. However, the upgrading from V4 to V6 might have caused a slightly greater impact on WB than W based on the magnitude of a ratio of the bias (difference between V6 and V4) to the V4 mean. Accordingly, WB has a ratio of 1.51% (0.015:0.995) that is greater than 0.49% (0.22:45.36) of W.

The daily Qair retrieved based on W and WB from the respective SSM/I V6 and V4 are also compared against the observed Qair from the five experiments altogether. The retrieved humidity using the upgraded V6 is found with a slightly improved correlation (0.86) and yet a higher bias (0.82 g kg-1) than those of V4 (0.85 and 0.59 g kg-1, respectively). The quantitative (ratio) analysis applied for W and WB

is also performed for Qair. The ratio of the increased bias in Qair (0.23 g kg-1, i.e., from 0.59 g kg-1 of V4 to 0.82 g kg-1 of V6) to the mean Qair of V4 (18.25 g kg-1) is 1.26%, which is considerably closer to that of WB (1.51 %) than that of WB (0.49 %). It confirms that the retrieved specific humidity highly depends on the water vapor in the lower part of PBL, i.e., WB.

4.3 Quality Control and Diagnostics

The newly produced GSSTF2b fluxes, i.e., SHF, LHF and τ, along with their counterparts from GSSTF2, have been validated against the ship measurements from the aforementioned five 1999 experiments (Figs. 1-3). It is found that the GSSTF2b product generally agrees better with the observations than its counterpart (GSSTF2) does in all three flux components. All three flux quantities of GSSTF2b are found with a higher/better correlation than those of GSSTF2. Note that "GO" (in green) represents the fluxes produced by directly applying the observational input parameters into the GSSTF model. As expected, "GO" possesses the best statistics (compared to both GSSTF2b and GSSTF2) that suggests two features. First, it ensures us a fine and physical-consistent GSSTF model. It also implies that there is still a room for us to continue thriving for acquiring more realistic and reliable input datasets/parameters besides improving our retrieval scheme. Shie (2010) further likens the aforementioned scenario using his invented **"Rice Cooker Theory"**:

"To produce a bowl of delicious 'cooked rice' (useful and trustworthy 'output product') depends not only on a fine and working 'rice cooker' ('model/algorithm'), but also on good-quality 'raw rice' (genuine and reliable 'input data')."

Note that GSSTF2b consists of two major daily ("Combined") datasets, i.e., Set1 and Set2. The earlier produced dataset (Set1) by combining the produced fluxes from all the available satellites seemed to possess a slightly increasing trend in globally averaged latent heat flux (E) post year 2000. This slightly increasing trend in E is mainly due to a slightly decreasing trend in the SSM/I TB whose Tb19v and Tb22v channels having been used to retrieve the WB, and then produce the Qair, and eventually the E. The decrease in WB results in a decrease of Qair, then an increase of DQ (i.e., Qs-Qair), and E eventually. The WB trend, however, varies among different satellite tapes (i.e., F8, F10, F11, F13, F14 and F15) that some satellite retrievals tend to possess a relatively larger trend than the others at certain periods of time. The slightly decreasing trend shown in globally averaged SSM/I WB ("Combined") post 2000 was also found in an estimated WB time series (Feb 2000-Dec 2008) based on a vertically integrated MODIS water vapor from the surface to 920 mb. The magnitude of the retrieved SSM/I WB is relatively smaller than that of the approximated MODIS, though. Nonetheless, a second Combined dataset (Set2) was produced by subjectively removing some of the satellite retrievals for certain time periods that we believed possessed relatively higher global trend in E. Accordingly, Set2 contains a smaller global temporal trend in latent heat flux post 2000 than Set1 does, yet for being compromised by gaining more missing data due to involving less available satellite data. In the 21.5-year period (July 1987-Dec 2008), Set2 is the same as Set1 except for the following months and years:

Months in partial years: 199101, 199102, 199104; 199704, 199712; 200801~200807

Entire years: 1998, 1999, ... 2006, 2007

Regardless, the GSSTF2b fluxes, either Set1 or Set2, can genuinely demonstrate significant features/signatures of weather and climatological events such as El Niño/La Niña, monsoon, storm tracks and etc. The users should feel free to use either Set1 or Set2 with their own interests and justifications (likewise, the product from individual satellites should be freely used). Proper citations and references to be addressed in users' future journal and conference paper publications are recommended and appreciated.

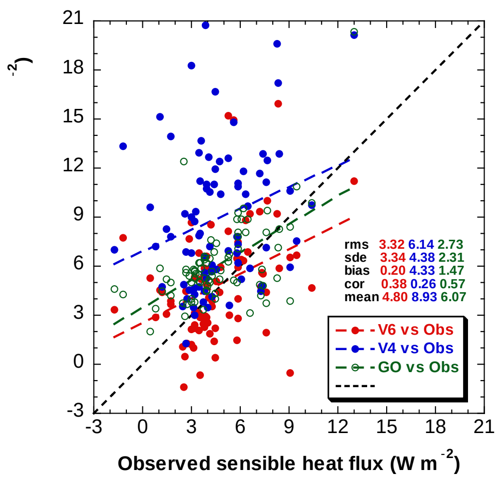

Figure 1: The respective GSSTF2b (based on combined F13 and F14 of SSM/I V6) (red solid circle) and GSSTF2 (based on combined F13 and F14 of SSM/I V4) (blue solid triangle) daily sensible heat flux vs. the observed from the five experiments altogether. The daily sensible heat flux ("GO") computed by applying ship data into the GSSTF bulk flux model vs. the observed is also shown (green open circle).

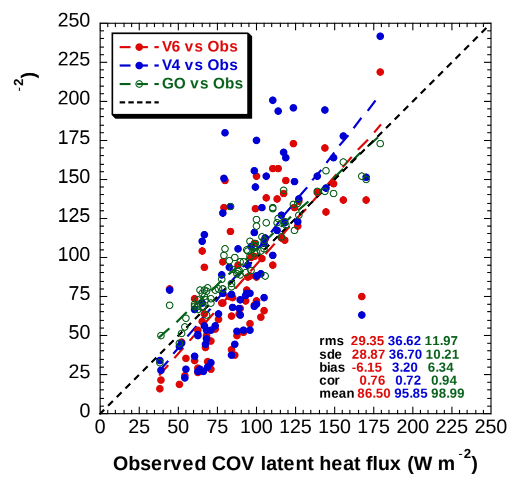

Figure 2: The respective GSSTF2b (based on combined F13 and F14 of SSM/I V6) (red solid circle) and GSSTF2 (based on combined F13 and F14 of SSM/I V4) (blue solid triangle) daily latent heat flux vs. the observed from the five experiments altogether. The daily latent heat flux ("GO") computed by applying ship data into the GSSTF bulk flux model vs. the observed is also shown (green open circle).

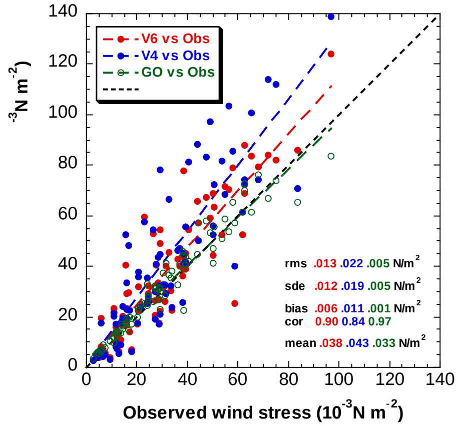

Figure 3: The respective GSSTF2b (based on combined F13 and F14 of SSM/I V6) (red solid circle) and GSSTF2 (based on combined F13 and F14 of SSM/I V4) (blue solid triangle) daily wind stress vs. the observed from the five experiments altogether. The daily wind stress ("GO") computed by applying ship data into the GSSTF bulk flux model vs. the observed is also shown (green open circle).

4.4 Algorithm Baseline Selection

The GSSTF bulk flux model (based on the surface layer similarity theory, Chou, 1993) used for performing the recently-produced/future production (GSSTF2b/GSSTF3) is essentially the same as that for GSSTF2 (Chou et al., 2003). Similar to GSSTF2, GSSTF2b requires the same methodology and same kinds of input data such as the surface/10-m wind speeds (U), total precipitable water (W), bottom-layer (500 m) precipitable water (WB), SST, 2-m air temperature (Ta), and sea level pressure (SLP). The air-sea turbulent fluxes, i.e., wind stress (τ), sensible heat flux (H), and latent heat flux (E) can be given in the following bulk aerodynamic formula:

$\tau = \rho \; CD \; (U–Us)^2$, (1a)

$H = \rho \; Cp \; CH \; (U–Us) \; (\theta s–\theta a)$, (1b)

$E = \rho \; L\upsilon \; CE \; (U–Us) \; (Qs–Qair)$, (1c)

where ρ is air density, Cp the isobaric specific heat, Lυ the latent heat of vaporization, CD, CH, CE the three respective bulk transfer coefficients, and Us is the negligibly small ocean surface current (about 0.55 of frictional velocity). The input parameters are the wind speed (U), the sea surface temperature (θs), the air potential temperature (θa), the specific humidity (Qair) at the reference height, and the saturation specific humidity (Qs) at the sea surface temperature.

Based on surface layer similarity theory, the surface fluxes in Eqs. (1a)-(1c) can also be derived from the scaling parameters for wind or friction velocity (u∗), temperature (θ∗), and humidity (q∗) as

$\tau = \rho\, u_*^2$, (2a)

$H = -\rho\, C_p\, u_* \theta_*$, (2b)

$E = -\rho\, L_\upsilon\, u_* q_*$ (2c)

For a given θs (or SST) and wind, temperature, and humidity at the measurement or reference heights within the atmospheric surface layer, the scaling parameters are solved through the roughness lengths and dimensionless gradients of wind, temperature, and humidity. The dimensionless gradients of wind, potential temperature, and humidity are functions of the stability parameter z/L, where z is the measurement height, and L the Monin–Obukhov length, which depends on the scaling parameters or fluxes (detailed description can be found in Chou et al. 2003). Accordingly, the transfer coefficients, which reflect the efficiency of the vertical transportation of momentum, heat, and moisture flux, are a non-linear function of the vertical gradient in wind speed, temperature and water vapor near the surface and, therefore, are affected by the stability of the surface air. Liu et al. (1979) performed detailed analysis of the transfer coefficients based on their model and predicted that under low wind conditions the transfer coefficient might increase with increasing wind speed, because the increased roughness facilitates the transfer of heat and vapor. However, as the wind speed increases further, the sheltering effect due to the troughs between waves becomes more significant and will suppress the exchange of vapor and heat. As the wind speed reaches about 5 m s^{-1}, the negative and positive effects due to increased wind speed counterbalance each other. If wind speed increases further, the transfer coefficient may even start to decrease. Latest field and laboratory measurements have shown that the drag coefficient does not increase with wind speed at extreme wind conditions, i.e., greater than 30 m s^{-1} (Powell et al., 2003; Donelan et al., 2004). High-wind transfer coefficients (based on Powell et al., 2003; Donelan et al., 2004; Black et al., 2007) may be applied for the 10-m winds beyond 18 m s^{-1} (or even higher) in our future production of GSSTF3. Such a high-wind treatment may improve the surface flux retrieval, as well as provide a better understanding of weather systems with high winds such as tropical cyclones, hurricanes and typhoons.

5 Constraints, Limitations and Assumptions

Similar to the previous GSSTF products (e.g., GSSTF2), the surface fluxes of GSSTF2b are limited to the global open-sea areas. Areas over continents/lands and the sea-ice covered oceans (i.e., high latitudes) are therefore filled with missing data.

As addressed earlier in section (4.1), WB derived from SSM/I TB, along with W, were used to retrieve surface air specific humidity (Qair) using the first two vertical EOFs of FGGEIIb humidity soundings of six W-based climatic regimes (Chou et al. 1995 and Chou et al. 1997). Two well-justified

modifications/constraints applied in the GSSTF EOF algorithm for retrieving surface humidity (Chou et al. 1997) are worth mentioning:

(1) Over the wintertime extratropical oceans the SSM/I surface humidity retrieved by Chou et al. (1995) was systematically underestimated for Q < 5 g kg^{-1}. The reason for the negative humidity bias was that the surface humidity depended highly on WB that was underestimated for low WB < 3 kg m^{-2}. To reduce the negative humidity bias for the drier climatic regimes, the SSM/I surface humidity derived highly based on WB would be replaced by that derived mainly based on W if the latter was larger. This modification is restricted to the situation with W < 20 kg m^{-2} and WB < 2.8 kg m^{-2} for the wintertime extratropical oceans while excluding the trade wind belts.

(2) In the summer, as the warmer continental (or maritime) air moves over a colder ocean surface, fog or stratus may form with the surface air reaching saturation at a temperature near the underlying cold SST. These areas are generally located over the extratropical oceans and the cold oceanic upwelling regions off the west coasts of North America, South America, and Africa during the summer. Under this situation, the original EOF method of humidity retrieval (Chou et al. 1995) tended to overestimate the surface humidity when fog or stratus forms. To reduce the positive humidity bias, the saturation specific humidity (Qs) of daily SSTs was used as an upper bound for the retrieval of SSM/I surface humidity.

In closing, we would like to reemphasize the importance of acquiring/using quality input datasets in the GSSTF flux production that is elaborated earlier via an analogy of "Rice Cooker Theory" (section 4.3). For example, the authenticity of the input SSM/I TB would affect the quality of the retrieved Qair and E, so does the authenticity of the input NCEP SST and Ta to the quality of the retrieved H. There is still a room for us to further improve our future GSSTF flux production by acquiring more and more genuine and reliable input datasets/parameters, along with a continual improvement/development in our model/scheme.

6 References

Atlas R., R. N. Hoffman, S. C. Bloom, J. C. Jusem, and J. Ardizzone, 1996: A multiyear global surface wind velocity dataset using SSM/I wind observations. *Bull. Amer. Meteor. Soc.*, **77**, 869–882.

Atlas R. M., J.V. Ardizzone, R. N. Hoffman, and J. C. Jusem, 2009: The cross-calibrated, multi-platform (CCMP) ocean surface wind product: Current status and plans. *The 2009 AGU Fall Meeting*, San Francisco, CA, December 14-18, 2009.

Black, P. G., E. A. D'Asaro, W. M. Drennan, J. R. French, P. P. Niiler, T. B. Sanford, E. J. Terrill, E. J. Walsh, and J. A. Zhang, 2007: Air-sea exchanges in hurricanes. *Bull. Amer. Meteor. Soc.*, 88, 357-374.

Chou, S.-H., 1993: A comparison of airborne eddy correlation and bulk aerodynamic methods for ocean-air turbulent fluxes during cold-air outbreaks. *Bound.-Layer Meteor.*, 64, 75-100.

Chou, S.-H., R. M. Atlas, C-L. Shie and J. Ardizzone, 1995: Estimates of surface humidity and latent heat fluxes over oceans from SSM/I data, *Monthly Weather Review,* **123**, 2405-2425.

Chou, S.-H., C.-L. Shie, R. M. Atlas, and J. Ardizzone, 1997: Air-sea Fluxes Retrieved from Special Sensor Microwave Imager Data, *Journal of Geophysical Research*, **102**, 12705-12726.

Chou, S.-H., E. Nelkin, J. Ardizzone, R. Atlas, and C.-L. Shie, 2001: The Goddard Satellite-Based Surface Turbulent Fluxes Dataset --- Version 2 (GSSTF 2.0) [global (grid of 1°x1°) daily air-sea surface fluxes from July 1987 to December 2000] distributed by Goddard DISC at http://disc.sci.gsfc.nasa.gov/precipitation/data-holdings/access/gsstf2.0.shtml/.

Chou, S.-H., E. Nelkin, J. Ardizzone, R. M. Atlas, and C.-L. Shie, 2003: Surface turbulent heat and momentum fluxes over global oceans based on the Goddard satellite retrieval, version 2 (GSSTF2). *J. Climate*, 16, 3256-3273.

Curry, J. A. and Coauthors, 2004: SEAFLUX, *Bull. Amer. Meteor. Soc.*, **85**(3), 424.

Donelan M. A., B. K. Haus, N. Reul, W. J. Plant, M. Stiassnie, H. C. Graber, O. B. Brown, and E. S. Saltzman, 2004: On the limiting aerodynamic roughness of the ocean in very strong winds, *Geophys. Res. Lett.*, **31**, L18306.

Kubota, M., K. Ichikawa, N. Iwasaka, S. Kizu, M. Konda, and K. Kutsuwada, 2002: Japanese Ocean Flux Data Sets with Use of Remote Sensing Observations (J-OFURO). *J. Oceanogr.*, **58**, 213–215.

Liu W. T., K. B. Katsaros, and J. A. Businger, 1979: Bulk parameterization of air-sea exchanges of heat and water vapor including the molecular constraints at the interface. *J. Atmos. Sci.*, **36**, 1722–1735.

Powell, M. D. P. J. Vickery, T. A. Reinhold, 2003: Reduced drag coefficient for high wind speeds in tropical cyclones, *NATURE*, **422**, 279-283.

Schulz J., P. Schluessel, and H. Grassl, 1993: Water vapor in the atmospheric boundary layer over oceans from SSM/I measurements. Int. J. Remote Sens., **14**, 2773–2789.

Schulz, J., J. Meywerk, S. Ewald, and P. Schluessel, 1997: Evaluation of satellite-derived latent heat fluxes. *J. Climate*, **10**, 2782–2795.

Shie, C.-L., L. S. Chiu, R. Adler, E. Nelkin, I-I Lin, P. Xie, F.-C. Wang, R. Chokngamwong, W. Olson, and D. A. Chu, 2009: A note on reviving the Goddard Satellite-Based Surface Turbulent Fluxes (GSSTF) dataset. *Adv. Atmos. Sci.*, **26**, No. 6, 1071-1080.

Shie, C.-L., L. S. Chiu, R. Adler, S. Gao, R. Chokngamwong, I-I Lin, E. Nelkin, J. Ardizzone, P. Xie, and F.-C. Wang, 2010: A recently revived and produced global air-sea surface turbulent fluxes dataset – GSSTF2b: Validations and Findings. *Proceedings of the Joint 2010 CWB Weather Analysis and Forecasting & COAA 5th International Ocean-Atmosphere Conference*, 307-312, Taipei, Taiwan, June 28-30, 2010.

Shie, C.-L., 2010: A recently revived dataset of satellite-based global air-sea surface turbulent fluxes (GSSTF2b) – features and applications. *The 17th Conf. on Sat. Meteor. and Oceanog.*, 27 September – 1 October 2010, Annapolis, MD. (Keynote speech)

Woodruff, S. D., S. J. Lubker, K. Wolter, S. J. Worley, and J. D. Elm, 1993: Comprehensive Ocean-Atmosphere Data Set (COADS) release la: 1980–92. *Earth System Monitor*, **4**, 4–8.

Xing, Yukun, 2006: Recent changes in oceanic latent heat flux from remote sensing, Ph.D. Dissertation, School of Computational Science, George Mason University, Fairfax VA 22030, 119 pp.